Soil–Building Interaction Analysis with Nearby Water Body, Based on an Input Wavefield

Masahiro Iida, A.M.ASCE[1]

Abstract: In this article, a three-dimensional (3D) linear finite-element method with an included water volume for examining the soil–building interaction based on a three-component input seismic wavefield is presented. A seismic wavefield means seismic waves propagating in a 3D medium. The method was constructed with the goal of adequately treating seismic surface waves trapped by a deep (several kilometers) underground structure in a soil–building interaction system. Surface waves play an important role in a soft sediment where the amplitudes increase strongly. In the new method, very soft soils are substituted for the water volume so that only solid material is treated, and wave propagation is controlled according to wave types in the very soft soils that replace the water volume. The method is applied to the reclaimed zone of Tokyo Bay to explore the effects of the water volume on soil and building responses. The method seems to work fairly well, showing that the soil responses become more variable and the building responses get larger because of the water volume. **DOI: 10.1061/(ASCE)GM.1943-5622.0001168.** *© 2018 American Society of Civil Engineers.*

Author keywords: Structural dynamics; Three-dimensional analysis; Concrete structures; Soil–structure interactions; Water; Water waves; Wave propagation; Underground structures.

Introduction

It is a common recognition that heavy seismic damage tends to occur in specific areas along a river or a coastline in an alluvial plain. One of the major reasons is that a soft surface deposit is present along a river or a coastline, and ground motions get captured and amplified in a soft surface deposit. Conversely, it is questionable whether a nearby water body itself affects ground motions. The effects of the water itself are uncertain because such an estimate has not been made. In short, a lack of such an estimate prevents us from understanding the seismic damage pattern. This question motivated the present study, which aimed to estimate the effects of the water itself on ground motions.

The seismic dynamic behavior of artificial structures closely associated with water has been investigated mainly in regard to dams and tanks. These investigations have been developed over the past several decades. A considerable number of studies regarding dams and similar structures were performed by Chopra (1968), Antes and Estorff (1987), Abdel-Ghaffar and Elgamal (1987), Miura and Wang (1993), and others. Those studies tried to take the substantial effects of water into account. The orthodox technique for treating dams is to construct a wave equation for the water volume and combine the wave equation with an equation of motion for the solid volume [e.g., Shiojiri and Taguchi (1985); Touhei and Ohmachi (1990)]. As for tanks, studies [e.g., Housner (1963); Jaiswal et al. (2007); Larkin (2008); Matsui and Nagaya (2015)] have investigated the sloshing of liquid for a large tank with various mathematical techniques. Recently, various types of interaction analyses related to water were performed [e.g., Shija and MacQuarrie (2015); Sheil and Finnegan (2017)].

Although the inherent modeling and treatment of these structures are very suitable, they are not applicable to other types of structures associated with water. Also, although the identification of wave types of ground motions is necessary in some response analyses, it has not been done because of the extreme difficulty in the short-period range (less than a few seconds). For this situation, the present study attempts to reveal the effects of a nearby water body on soil and building responses. This attempt is carried out using a new method with an included water volume for examining the soil–building interaction. In the new method, very soft soils are substituted for the water volume so that only solid material is treated, and wave propagation is controlled according to wave types in the very soft soils that replace the water volume.

Soil–building interaction analysis has only a short history. It was initiated in the 1950s [e.g., Housner (1957)] and became popular in the 1970s [e.g., Flores-Berrones and Whitman (1982); Bielak and Christiano (1984)]. It is of great benefit to estimate the seismic response of a building reasonably. In an interaction analysis, in addition to interaction effects, not only building modes but also soil modes of vibration can be taken into account, and body waves can be treated properly.

However, in an interaction analysis, it is very difficult to treat short-period surface waves reasonably because surface waves can be trapped by a deep (several kilometers) underground structure. Here, an underground structure means an existing underground geotechnical structure. The vertical increase in the amplitude of short-period surface waves in a shallow (several tens of meters) underground structure depends strongly on the material properties of the deep structure in which the surface waves propagate. This means that surface-wave incidence in a shallow soil model is not valid for surface waves trapped by a deep structure. This problem of surface waves was explained mathematically in a soil-response study by Iida (2006). Short-period surface waves play an important role in a soft sediment where the amplitudes increase strongly.

To treat short-period surface waves adequately in a building-response analysis, a three-dimensional (3D) linear finite-element

[1]Earthquake Research Institute, Univ. of Tokyo, 1-1-1 Yayoi, Bunkyo-ku, Tokyo 113-0032, Japan. E-mail: iida@eri.u-tokyo.ac.jp

Note. This manuscript was submitted on August 1, 2017; approved on December 19, 2017; published online on April 3, 2018. Discussion period open until September 3, 2018; separate discussions must be submitted for individual papers. This paper is part of the ***International Journal of Geomechanics***, © ASCE, ISSN 1532-3641.

(FE) method for examining the soil–building interaction based on a horizontal-component input seismic wavefield was proposed (Iida 2013). An input seismic wavefield means that the forces produced by body and surface waves propagating in the 3D soil volume of a soil–building interaction system are employed as external forces in the FE simulations, which is described mathematically in the section on methods. The proposed approach makes it possible to estimate building responses induced by surface waves in a sufficiently wide period range within the framework of a soil–building interaction system. Using the proposed method, the seismic responses of low- to high-rise RC model buildings were successfully calculated for a large earthquake at a soft-soil site in Mexico City, where surface waves are very dominant.

The horizontal-component input seismic wavefield was extended to a three-component one in a recent soil-response study (Iida 2016). In the extension, the identification of wave types in constructing a vertical-component wavefield was found to be much more difficult than that in constructing a horizontal-component wavefield. Also, the vertical soil responses were overpredicted considerably because of insufficient treatment of artificial reflections of vertical ground motions on the boundaries of the soil model. Nevertheless, FE-simulated soil responses based on the three-component input seismic wavefield successfully clarified that vertical ground motions affect soil responses very little in the usual situation that vertical accelerations do not exceed gravity.

The construction of a three-component input seismic wavefield enabled the development of the new method in the present study. The strong point of the new method is the adequate treatment of seismic waves not only in the solid volume but also in the water volume, using the three-component input wavefield. In the water, whereas some kinds of seismic waves [P waves and Rayleigh (gravity) waves] are able to propagate, other kinds of seismic waves (S waves and Love waves) are not able to propagate. This means that, as explained in the next section, roughly speaking, only vertical ground motions are able to propagate in the water. The new method considers these features of seismic waves properly.

The present study applies the 3D linear FE method with an included water volume to the reclaimed zone of Tokyo Bay to examine the validity of the method and explore the effects of the water volume on soil and building responses. In a multilayered soil model with an included water volume subject to both horizontal and vertical ground motions, the analysis is performed in the period range between 0.2 and 5.0 s. The analysis can be made using the three-component input wavefield that identifies the kinds of seismic waves on the basis of the aforementioned previous studies. The validity of the method is demonstrated using strong-motion recordings. For reference, many soil–building interaction analyses that treat neither surface waves nor water volumes have been conducted in the Tokyo metropolitan area, including the reclaimed zone [e.g., Ohta et al. (1978); Abe et al. (1984)].

Methods

This section explains the 3D linear time-domain FE method with an included water volume for examining the soil–building interaction based on a three-component input seismic wavefield. The new method, which is basically the same as the original method without a water volume based on only a horizontal-component input wavefield (Iida 2013; Iida et al. 2015) in the mathematical formulation, requires a vertical-component input wavefield and additionally the adequate treatment of seismic waves in the water volume. In the new method, although the soil–building interaction system is standard (Iida 2013; Iida et al. 2015), the treatment of seismic waves is very unique, using the three-component input wavefield that identifies the kinds of seismic waves (Iida 2016). The treatment of seismic waves in the water volume is also standard on the basis of wave theory. In the following discussion, the fundamentals and the incremental advances of the new method are described.

Fig. 1 illustrates the 3D superstructure–foundation–pile–soil systems for three cases treated in the present study, together with deep underground structures used to estimate input wavefields. The interaction systems are the same as those employed in previous interaction studies (Iida 2013; Iida et al. 2015). The lumped-mass stick building superstructure rested on a rigid box foundation supported on piles. The superstructure was modeled as a shear spring system, and sway and rocking of the foundation were considered. The horizontal degree of freedom of each story was coupled with the rocking degree of freedom at the foundation.

Each pile was modeled by beam elements, and the soil volume was modeled by 3D rectangular prism elements. To allow the relative movement of the pile with respect to the soil, a joint spring element, which connects a node for the soil and another node for the soil, was attached to both edges of each beam element that forms the pile. The side and bottom boundaries of the soil volume were equipped with viscous dampers, which are able to reproduce the transmission of body waves propagating normal to the boundary (Lysmer and Kuhlemeyer 1969). The viscous dampers work moderately for surface waves and vertical ground motions (Iida 2016). Prior to the dynamic calculation, initial strains and stresses of the piles and the soil were evaluated by a static gravity load analysis. In the dynamic calculation, the evaluated initial stresses were supplied, thereby taking gravity into account.

In the new method, very soft soils are substituted for the water volume, so that only solid material is treated. Consequently, the equation of motion that connects the superstructure, the foundation, the piles, and the soil is represented by the following formulation:

$$
\begin{aligned}
&[M]\,\{\delta^2\chi_a/\delta t^2\,\delta^2\chi_b/\delta t^2\,\delta^2\chi_c/\delta t^2\,\delta^2\chi_d/\delta t^2\,\delta^2\chi_e/\delta t^2\}^T \\
&\quad+[C]\,\{\delta\chi_a/\delta t\,\delta\chi_b/\delta t\,\delta\chi_c/\delta t\,\delta\chi_d/\delta t\,\delta\chi_e/\delta t\}^T \\
&\quad+[K]\,\{\chi_a\,\chi_b\,\chi_c\,\chi_d\,\chi_e\}^T=\{F_a\,F_b\,F_c\,F_d\,F_e\}^T \qquad (1)
\end{aligned}
$$

where $[M]$ = mass matrix; $[C]$ = damping matrix; $[K]$ = stiffness matrix; $\{\chi\}$ = displacement vector associated with the system; $\{F\}$ = external force vector; and t is time. The superscript T denotes the transposed vector, and subscripts a, b, c, d, and e correspond to the superstructure, the foundation, the piles or the soil body, the side boundaries of the system, and the bottom boundary of the system, respectively. The equation of motion is solved by the Newton–Raphson technique.

The three-component wavefield estimation based on wave theory is described in detail in a recent study (Iida 2016). At the beginning of the estimation, for the kth layer of a multilayered structure in 3D (x, y, z) coordinates, the wave equation for S waves and/or Love waves is expressed by

$$\rho_k\delta^2\zeta/\delta t^2=\mu_k\Psi^2\zeta \qquad (2)$$

and the wave equation for P waves and/or Rayleigh waves is expressed by

$$\rho_k\delta^2\eta/\delta t^2=(\lambda_k+\mu_k)\delta\Delta/\delta x+\mu_k\Psi^2\eta \qquad (3a)$$

$$\rho_k\delta^2\theta/\delta t^2=(\lambda_k+\mu_k)\delta\Delta/\delta z+\mu_k\Psi^2\theta \qquad (3b)$$

Int. J. Geomech., 2018, 18(6): 04018053

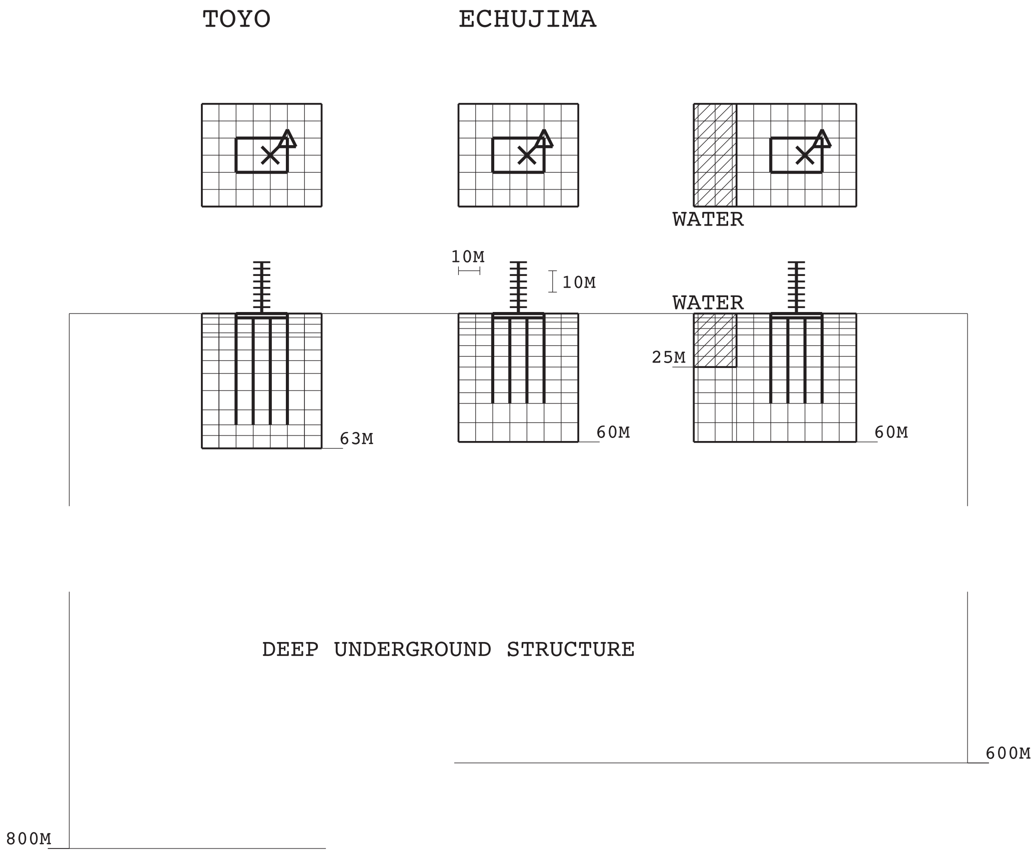

Fig. 1. Plan sections and cross sections (east–west direction) of the 3D superstructure–foundation–pile–soil systems for the three cases (Note: The cross on the cross section shows the vertical line where soil responses are computed; the triangle indicates the corner pile where the maximum bending moments are evaluated; 1D appropriate deep underground structures used to estimate input wavefields are also displayed)

where ζ and η = horizontal displacements; θ = vertical displacement; ρ = density; λ and μ = Lame's constants; t = time; $\Delta = \delta\eta/\delta x + \delta\theta/\delta z$; and $\Psi^2 = \delta^2/\delta x^2 + \delta^2/\delta z^2$.

In the present method, in the wavefield estimation, the water volume is replaced by the shallow multilayered underground structure in the land zone (Fig. 1). Vertically propagating plane body waves and horizontally propagating plane surface waves are imposed on the soil volume of the 3D (x, y, z) system. Then, the external force vector is expressed by

$$\{F_a\, F_b\, F_c\, F_d\, F_e\}^T = [M]\Big\{0\; \delta^2 p_b/\delta t^2 + \delta^2 q_b/\delta t^2\; \delta^2 p_c(z)/\delta t^2 + \delta^2 q_c(x,y,z)/\delta t^2\; \delta^2 p_d(z)/\delta t^2 + \delta^2 q_d(x,y,z)/\delta t^2\; \delta^2 p_e/\delta t^2 + \delta^2 q_e(x,y)/\delta t^2\Big\}^T \quad (4)$$

where p and q = external displacements contributed by body waves and surface waves in the soil volume of the system, respectively. The p and q terms are computed on the basis of Eqs. (3*a* and *b*) and (4) in Iida (2016). The evaluated response acceleration $\delta^2\chi/\delta t^2$ is the absolute response acceleration.

A body wavefield and a surface wavefield are separately estimated in the soil volume by applying elastic wave theory to an appropriate deep underground structure after surface ground motions are separated into body waves and surface waves. The whole wavefield used as input is the summation of the two wavefields. It is simply assumed that horizontal ground motions are composed of S waves and Love waves and that vertical ground motions are composed of P waves and Rayleigh waves.

The damping matrix of the new method was constructed in Iida et al. (2015), and the following spatially variable Rayleigh-type damping matrix is employed:

$$[C] = 2\omega_1[H_M]\,[M] + 2/\omega_1[H_K]\,[K] \quad (5)$$

where $[H_M]$ and $[H_K]$ = matrices of the damping factors associated with the mass and the stiffness, respectively; and ω_I = primary angular frequency of the ground. Here, $h_{WFij} = h_{Mij} = h_{Kij}$ is assumed, where h_{Mij} and h_{Kij} are the elements that lie in the ith row and in the jth column of the matrices $[H_M]$ and $[H_K]$, respectively. The spatially variable damping factors h_{WF} are determined experimentally so as to reproduce the wavefield by soil responses well. The actual evaluation is explained in a later section.

In liquid material, because μ is zero in Eqs. (2) and (3*a* and *b*), S waves and Love waves are absent. Hence, concerning S waves and Love waves, no input acceleration wavefield should be imposed in the water volume replaced by very soft soils. Accordingly, no acceleration soil responses should be produced in the water volume. To express these features of seismic waves properly, no input accelerations are given at the nodes inside the water volume. Besides, when possible, the soil responses are constrained to have no accelerations at the nodes inside the water volume. The soil-response constraint is possible on the condition that a component of the three-component input wavefield consists of either S waves or Love waves or both.

In the present study, the soil-response constraint is available for the two horizontal components.

The aforementioned three-component input wavefield is estimated approximately in the water volume replaced by very soft soils and in the soil volume that surrounds the water volume. The approximations hold roughly for the following reasons [e.g., Iida (2016)]. First, in the water volume, the horizontal components of ground motions are absent in the soil-response analysis, and the vertical components are not very sensitive to the assumed (liquid or solid) material. Second, in the soil volume that surrounds the water volume, in the case of vertically propagating body waves, the behavior of body waves in the surface layers is determined by only the material properties of the surface layers, so body waves are little influenced by the water volume. In the case of horizontally propagating surface waves, the high energy of surface waves in the surface layers is supplied from a deep underground structure in which surface waves are trapped, so surface waves are kept in much the same status regardless of the water volume.

Soil Responses

This section describes a soil-response analysis conducted by the new method to examine the validity of the method and explore the effects of the water volume on soil responses. The validity is demonstrated using strong-motion recordings obtained at two borehole stations. The soil-response analysis was performed for the Toyo and the Echujima borehole stations located in the reclaimed zone of Tokyo Bay for the 1923 Kanto earthquake (earthquake magnitude $M_J = 8.1$) (Fig. 2). Here, M_J means the magnitude determined by the Japanese Meteorological Agency. It is well known that the Tokyo metropolitan area suffered the heaviest seismic damage from the Kanto earthquake.

There are a lot of small rivers and canals in the reclaimed zone. Whereas the Toyo station is somewhat off the coastline, the Echujima station faces Tokyo Bay on the west side, and there is also a canal on the south side of the station. The shallow underground structure in the reclaimed zone varies from site to site, and it can be inferred that the shallow structure around the Echujima station is more heterogeneous than that around the Toyo station because of the waterside location. In the coastal environment, free soil

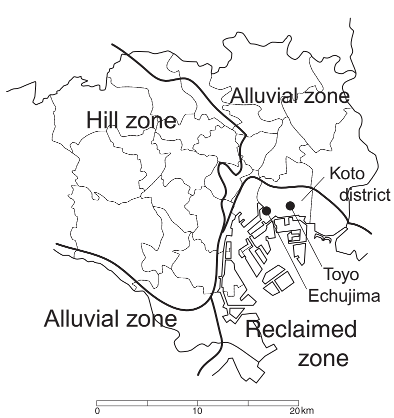

Fig. 2. Local map of the Tokyo metropolitan area (Note: The metropolitan area occupies the eastern parts of Tokyo prefecture and consists of the 23 districts delineated by fine lines; geotechnically, the metropolitan area is divided into the hill, the alluvial, and the reclaimed zones; the Toyo and Echujima borehole stations are located in the reclaimed zone and are indicated by filled circles)

responses were evaluated for three cases: (1) the Toyo station case, (2) the Echujima station case, and (3) the Echujima station case with a water volume (Fig. 1). Whereas the water-volume model represents a gross characteristic of the coastal environment, the actual 3D extent of the water volume is quite complex.

Input Wavefield

Prior to a soil-response analysis, an input wavefield was estimated for a large earthquake using an appropriate deep, multilayered structure (Fig. 1). The methodology is the same as that employed in a recent soil-response study (Iida 2016), where the same earthquake-station pairs as the present study were employed. The methodology is composed of three steps: (1) the wave type identification and the waveform separation in surface recordings from small earthquakes, (2) the waveform synthesis of each wave type on the ground surface for a large earthquake, and (3) the wavefield construction of each wave type for a large earthquake.

In the first step, the nature of ground motions was investigated for surface and borehole recordings from small earthquakes, and surface recordings were separated into some wave types. Practically, in two ground-motion studies (Iida et al. 2005; Iida 2007) conducted at the two borehole stations employed in the present study, the nature of ground motions was comprehensively investigated with various techniques. Accordingly, the horizontal components of surface accelerograms were separated into S waves and Love waves, and the vertical components were separated into P waves and Rayleigh waves.

In the second step, for a large earthquake, the surface accelerograms of each wave type were independently synthesized from the separated accelerograms, using an empirical Green's function summation technique. The mathematical expression of the summation technique used here is given in Iida (2006). In the technique, surface accelerograms of a large earthquake at a site were obtained from those of small earthquakes at the same site, considering the fault rupture of the large earthquake. The target large earthquake was the 1923 Kanto earthquake. Because the Toyo station has no vertical-component sensor, the author made use of the vertical component of the synthesized surface accelerograms at the Echujima station alternatively.

In the third step, the wavefield of each wave type was independently constructed for a large earthquake by applying elastic wave theory to an appropriate deep, multilayered structure on the basis of the synthesized surface accelerograms. The whole wavefield used as input was the summation of the estimated wavefields. The deep, multilayered structural models are listed in Tables 1 and 2. Here, the wavefield for Rayleigh waves could not be calculated using the original structural models, presumably because of calculation instability due to the large velocity variations in the extremely thin surface layers. Hence, in the case of Rayleigh waves, smoothed structural models were adopted in place of the original ones (Tables 1 and 2).

The constructed input wavefields are not presented here because they are reproduced well as linear soil responses. Up to now, wavefields have always been reproduced well as linear soil responses [e.g., Iida (2006, 2016)]. For reference, the wavefields at the Echujima station for the 1923 Kanto earthquake, which were estimated with a very similar deep, multilayered structural model to that employed in the present study, were displayed in a recent soil-response study (Iida 2016). According to the aforementioned two ground-motion studies, the predominant period of ground motions at the Echujima station is a little shorter than that at the Toyo station. Also, ground motions at the Echujima station contain more surface waves (Love waves) than do those at the Toyo station. At the

Table 1. Deep, Multilayered Structural Model Used at the Toyo Borehole Station

Model	Depth (m)	P-wave velocity (m/s)	S-wave velocity (m/s)	Density (ton/m^3)
Original model	0.0–2.0	800	280	1.45
	2.0–5.0	800	280	2.00
	5.0–9.0	1,100	160	1.75
	9.0–11.0	800	90	1.70
	11.0–17.0	1,050	90	1.50
	17.0–20.0	1,050	145	1.50
	20.0–24.0	1,150	190	1.50
	24.0–27.8	1,150	190	1.65
	27.8–32.0	800	230	1.55
	32.0–36.5	800	250	1.65
	36.5–45.4	1,300	250	1.55
	45.4–51.0	1,500	350	1.75
	51.0–63.2	1,500	290	1.75
	63.2–71.7	1,950	460	2.00
	71.7–90.0	1,500	410	1.95
	90.0–210.0	1,850	450	1.90
	210.0–800.0	1,830	880	1.90
	800.0–	1,830	880	1.90
Smoothed model	0.0–17.5	1,100	160	1.75
	17.5–27.9	1,150	190	1.60
	27.9–44.6	1,100	250	1.60
	44.6–63.2	1,500	290	1.75
	63.2–90.0	1,500	410	1.85
	90.0–210.0	1,850	450	1.90
	210.0–800.0	1,830	880	1.90
	800.0–	1,830	880	1.90

Note: To estimate a wavefield, a period-dependent damping factor is used, which was explained in a ground-motion study (Iida 2007). The smoothed model is used for only the calculation of Rayleigh waves.

Table 2. Deep, Multilayered Structural Model Used at the Echujima Borehole Station

Model	Depth (m)	P-wave velocity (m/s)	S-wave velocity (m/s)	Density (ton/m^3)
Original model	0–4	620	110	1.70
	4–10	940	110	1.70
	10–16	1,330	130	1.60
	16–25	1,330	130	1.70
	25–33	1,330	230	1.70
	33–38	930	230	1.70
	38–49	1,750	440	2.00
	49–60	1,750	440	1.90
	60–70	1,750	440	1.85
	70–75	1,750	300	1.85
	75–83	1,750	460	1.85
	83–100	1,750	460	1.90
	100–210	1,830	500	1.90
	210–600	1,830	880	1.90
	600–	1,830	880	1.90
Smoothed model	0–10	1,330	160	1.70
	10–26	1,330	180	1.70
	26–38	1,330	230	1.70
	38–60	1,750	440	2.00
	60–75	1,750	440	1.85
	75–100	1,750	460	1.90
	100–210	1,830	500	1.90
	210–600	1,830	880	1.90
	600–	1,830	880	1.90

Note: See Table 1 for the explanations.

Echujima station, surface waves are dominant rather than S waves around the predominant period. Furthermore, larger amplitudes of ground motions at the Echujima station than those at the Toyo station are attributed to more inclusion of surface waves.

Soil Responses from Input Wavefield

A soil-response analysis was conducted using the 3D interaction systems without a building (Fig. 1). For the water volume, the following parameter values were adopted: the P-wave velocity Vp = 1,430 m/s, the S-wave velocity Vs = 30 m/s, the density ρ = 1.1 g/cm^3, and the damping factor h_{WF} = 0.01. The depth of the rectangular prism model for the water volume was set as 25 m because the average water depth is 25 m or so in the inner Tokyo Bay. In the present study, the soil and building-response analyses were performed for 80 s with a time interval of 0.01 s and were valid at periods greater than 0.2 s.

Figs. 3 and 4 display the horizontal-component FE-simulated soil responses based on the input wavefields at the Toyo station and the Echujima station, respectively. They were obtained in the configuration without the water volume. Fig. 5 displays those at the Echujima station, which were obtained in the configuration with the water volume. These soil responses were computed at almost the central position of the building (Fig. 1), although the building was removed from the 3D systems in the soil-response analysis.

The spatially variable damping factors were determined by trial and error to reproduce the wavefield by soil responses well. At each station, an identical value was assigned to the upper soft layers, and another identical value was assigned to the other layers. At the Toyo station, whereas a damping factor h_{WF} of 0.05 was used for the soil layers above 28 m depth, another damping factor h_{WF} of 0.02 was used for those below 28 m depth. As a result, a reproduction of the horizontal-component input wavefield was achieved fairly well as a whole (Fig. 3). At the Echujima station, given a damping factor h_{WF} of 0.05 for the soil layers above 25 m depth and another damping factor h_{WF} of 0.02 for those below 25 m depth, a good reproduction of the input wavefield was attained as well (Fig. 4). In these graphs, acceleration wave trains are shown in the soft-soil sediments (Tables 1 and 2).

The simulated soil responses are summarized as follows. First, the soil responses at the Echujima station were much larger than those at the Toyo station, having shorter-period components. This feature matches well with observed ground motions, which were explained in the last paragraph of the subsection on the input wavefield. Second, at the Echujima station, it turns out that the soil responses in the case with the water volume were different from those in the case without the water volume in the east–west direction along which the soil volume was changed to the water volume. In terms of the amplitudes, the soil responses in the former case got somewhat larger than those in the latter case. As for the frequency contents, because of the water volume, some ground motions were transformed into shorter-period components. Third, in the north–south direction, no noticeable distinctions were seen between the two cases without and with the water volume.

On the basis of these results, one possible interpretation can be addressed. It seems that when the water volume is present, the predominant periods and the amplitudes of ground motions get shorter and larger, respectively. This might suggest that unless the Echujima station is adjacent to Tokyo Bay, the soil responses are much the same as those at the Toyo station, and that, because of the

Int. J. Geomech., 2018, 18(6): 04018053

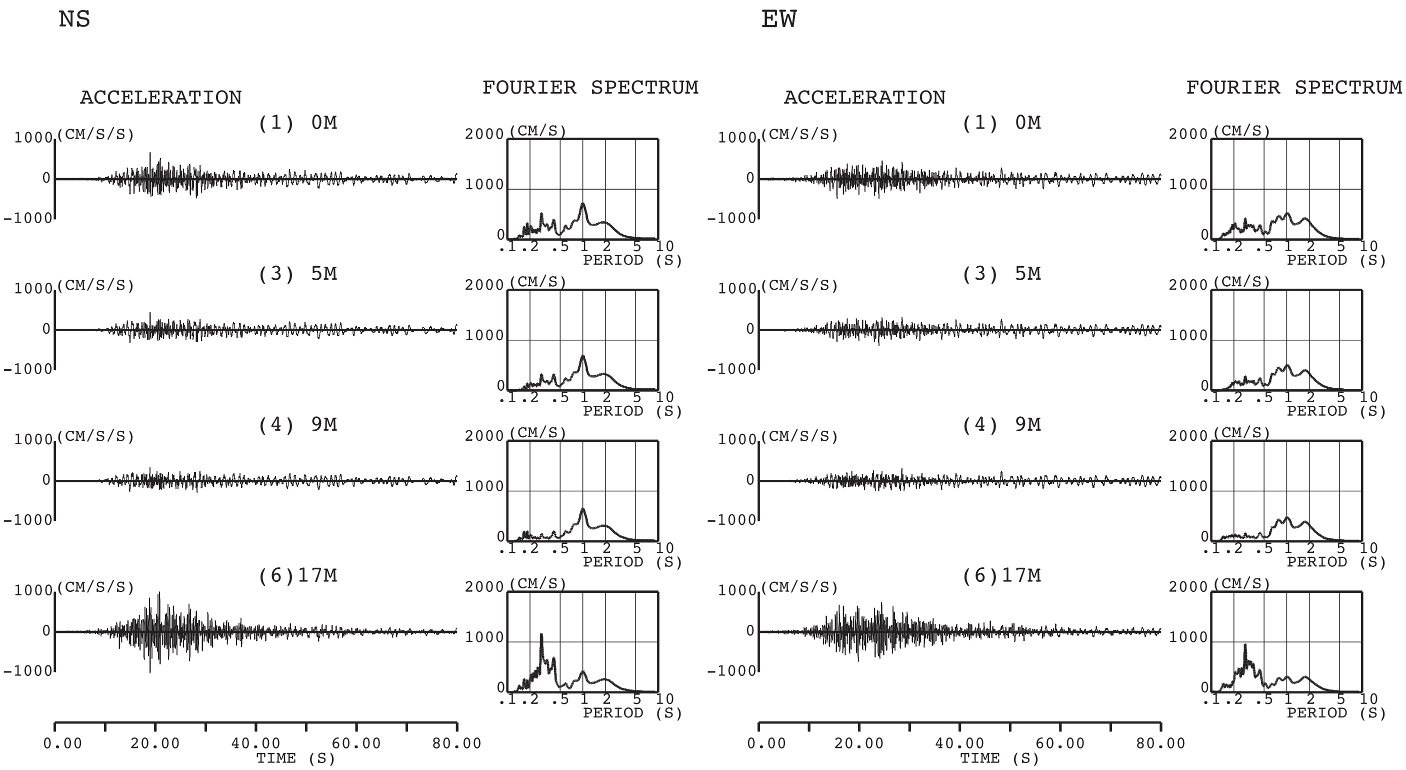

Fig. 3. Horizontal-component FE-simulated soil responses at four depths based on the input wavefield estimated at the Toyo station

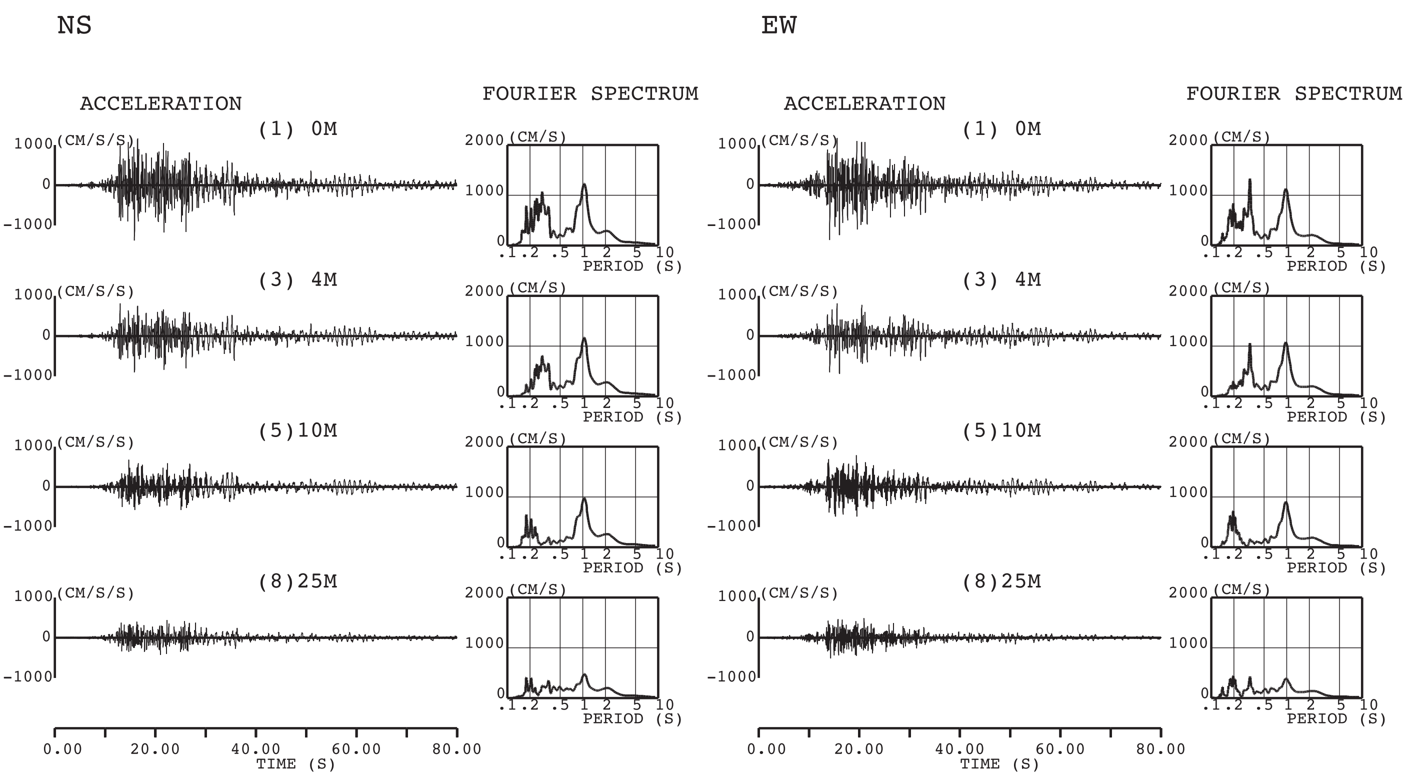

Fig. 4. Horizontal-component FE-simulated soil responses at four depths based on the input wavefield estimated at the Echujima station

water volume, they are altered to the FE-simulated soil responses based on the wavefield estimated from the observed recordings (Fig. 4). There is another interpretation. The shallow soil profiles (Tables 1 and 2) at the two stations are considerably different from each other. As a result of simply reflecting the differences in the profiles, the soil responses differ greatly between the two stations. It is concluded that either or both of these two interpretations should hold.

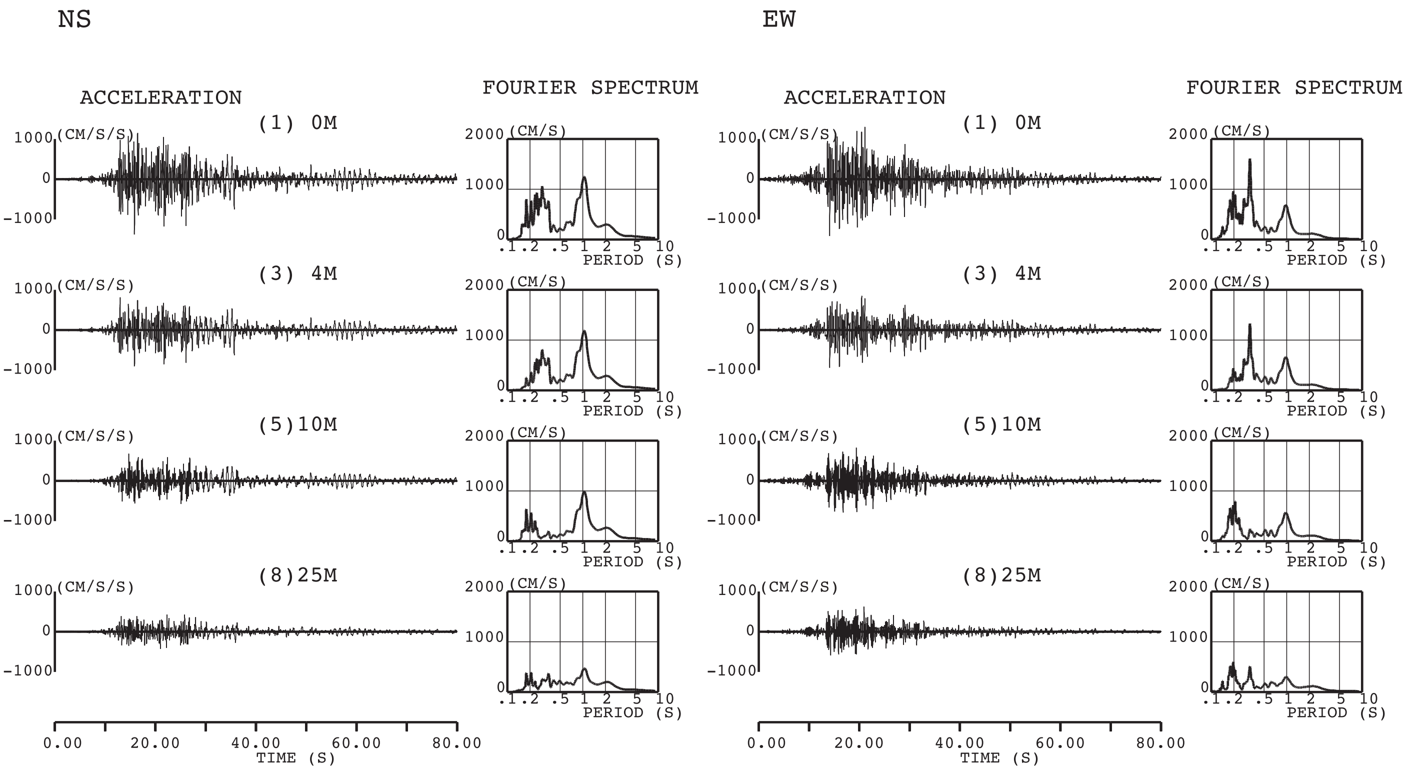

Fig. 5. Horizontal-component FE-simulated soil responses at four depths based on the input wavefield estimated at the Echujima station with a water volume

Building Responses

For more clarity on the effects of the water volume, this section investigates the seismic responses of an eight-story RC building calculated for the 1923 Kanto earthquake ($M_J = 8.1$) in the three cases, namely, the Toyo station case, the Echujima station case, and the Echujima station case with a water volume. A soil–building interaction analysis with a nearby water body is a very tough subject. It is almost impossible to carry out the analysis with existing techniques.

The 3D soil–building interaction systems for the three cases are shown in Fig. 1. In the Echujima station case with a water volume, an eight-story RC building is located very near the water volume. The RC building is a typical model building based on Japanese building codes (Building Center of Japan 2013) and was employed in a building-response study conducted in the reclaimed zone of Tokyo Bay (Iida et al. 2015). The parameters used for the superstructure and the foundation of the building are summarized in Table 3. The fundamental period was evaluated under a base-fixed condition. The parameters used for the piles of the building are summarized in Table 4. The horizontal stiffness of the joint spring element was set to be 10^9 kN·m, and the vertical stiffness was set to be 10^6 and 10^5 kN·m at the tip and other beam elements, respectively. These stiffnesses are the same as those employed in previous soil–building interaction studies (Iida 2013; Iida et al. 2015) and worked properly as well in the present study.

In the interaction analysis, a damping factor h_{WF} of 0.05 was assigned to the building. Fig. 6 plots the vertical distributions of the maximum interstory drift of the building for the three cases. Also, Fig. 7 plots the vertical distributions of the maximum bending moment of a corner pile of the building for the three cases. The location of the corner pile is displayed in Fig. 1. Please note that the bending moment in the north–south or east–west direction corresponds to the shear deformation in the east–west or north–south direction, respectively (Figs. 6 and 7).

It turns out that, as a whole, the building responses agree well with the soil responses obtained in the preceding section. At the Echujima station, as expected, the building responses were evidently affected by the water volume. The increase in the responses of both the superstructure and the piles due to the water volume was considerable. The large increase is attributed to the noticeable variation in soil responses in the east–west direction because the pile foundation had a certain extent in the horizontal directions (Fig. 1). It is considered that the building responses were evaluated properly.

Table 3. Parameters Used for the Superstructures and the Foundations of the Eight-Story RC Building

Part	Parameter	Value
Superstructure	Height of each story (m)	3.0
	Mass of each story (ton)	509
	Stiffness of each story (kN/m)	1.20×10^6 (4–8)
		1.23×10^6 (3)
		1.27×10^6 (2)
		1.66×10^6 (1)
	Yield shear strength of each story (kN)	4,988 (4–8)
		6,987 (3)
		9,290 (2)
		11,976 (1)
	Fundamental period (s)	0.68
Foundation	Mass (ton)	408
	Embedment (m)	2.0
	Length, width (m)	24, 16

Note: The numerical values inside the parentheses mean the story numbers.

Discussion

The new method basically seems to work well, and it is likely that the soil and building responses are reasonable. The obtained results give a distinct indication that the presence of a water volume changes soil responses and increases building responses. Additionally, the obtained results imply the potential capabilities of the new method. Inherent advantages of the new approach are summarized as follows: (1) The treatment of water volume is easy. (2) Multiple small water portions can be handled. (3) The approach is applicable to not only a RC building but also any artificial structure. (4) The approach can take material nonlinearity of the soil and the artificial structure into account, although a linear response analysis was performed in the present study.

There is an apparently contradictory report that inspected the effects of the seawater of Tokyo Bay on ground motions on a large scale (Iida and Hatayama 2007). The report demonstrated that the water layer of a typical model for shallow Tokyo Bay had little influence on ground motions with the water layer removed. In the report, the target site was 10 km away from the coastline. Conversely, in the present study, the effects of the seawater were recognized at a coastal site very close to the seawater (about 20 m). Therefore, the two opinions can stand together. A compatible interpretation of the two opinions might be that if the target site is away from the coastline to some extent, ground motions are free from the effects of the seawater.

Because the method is in the process of development, a few issues need to be examined. First, the approximate wavefields estimated in the water volume replaced by very soft soils and in the soil volume that surrounds the water volume might need some improvements. For example, Rayleigh waves might be largely amplified in the substituted very soft soils and might give an unfavorable influence on soil and building responses. Second, the soil–building interaction system with the water volume is greatly simplified and lacks a revetment for shore protection. The soil and building responses might become less sensitive to the effects of the water volume in the presence of a revetment. Third, the viscous dampers of the system do not work perfectly for surface waves and vertical ground motions. Other damping techniques such as a scaled boundary FE approach (Syed and Maheshwari 2014) might work better.

Table 4. Parameters Used for the Concrete-Filled Steel Piles of the Eight-Story RC Building

Parameter	Value
Number	12
Length (m)	50.0 (Toyo) 40.0 (Echujima)
Radius (m)	0.50
Elastic modulus (kN/m^2)	1.47×10^7
Density (ton/m^3)	2.4
Pure yield bending moment[a] (kN·m)	1,600
Maximum yield bending moment (kN·m)	2,600

[a]The pure yield bending moment means the yield bending moment without the axial force.

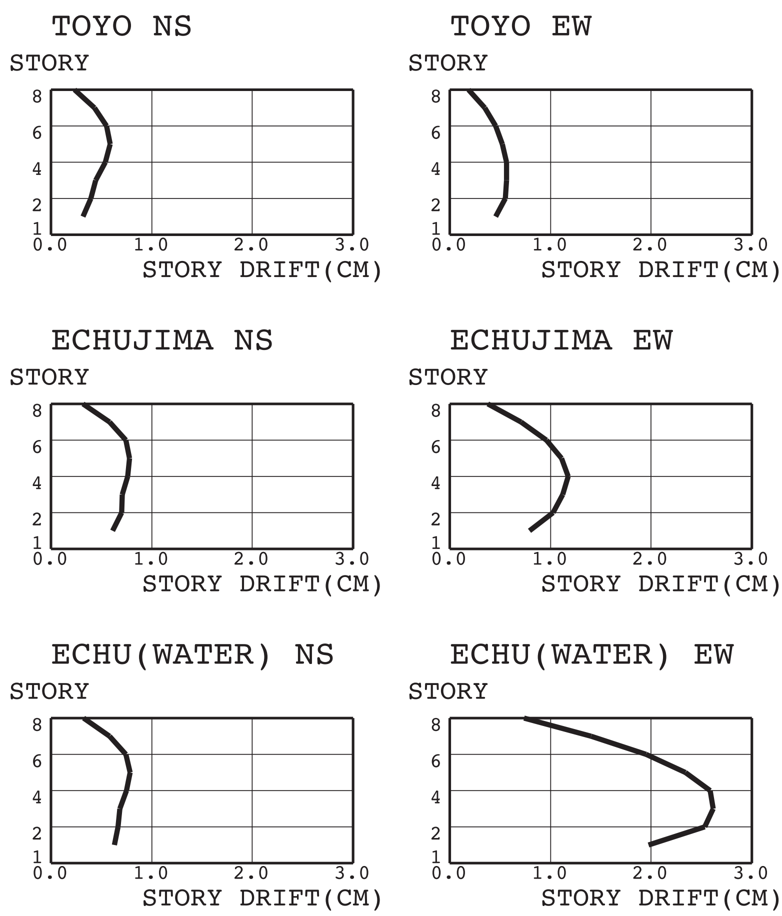

Fig. 6. Comparison of the vertical distributions of the maximum interstory drift of the eight-story RC building among the three cases

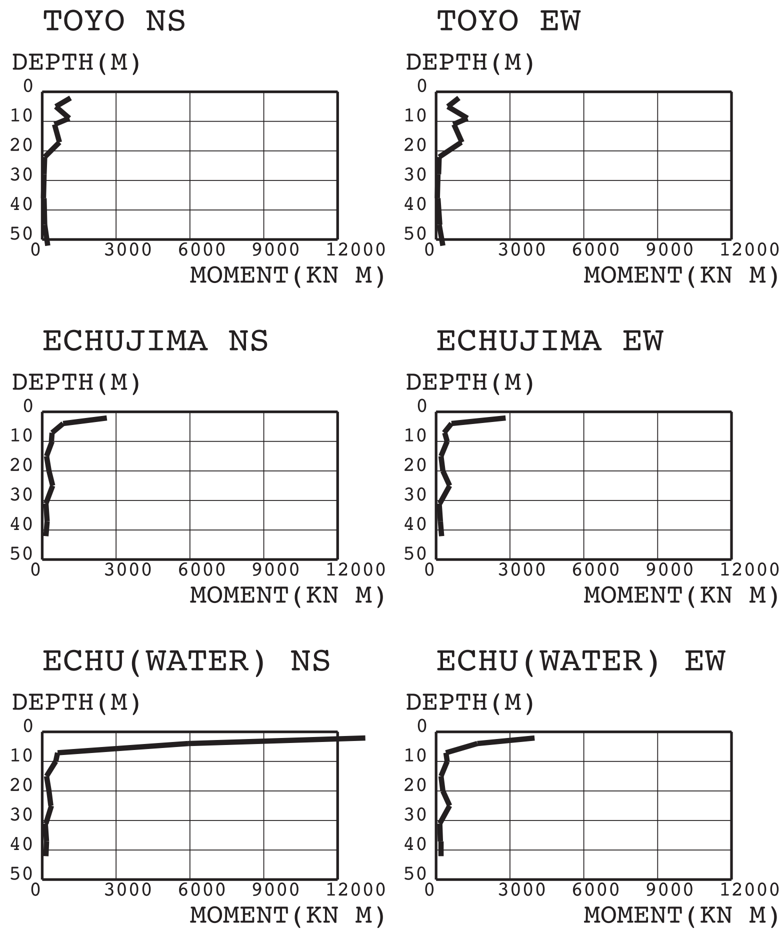

Fig. 7. Comparison of the vertical distributions of the maximum bending moment of a corner pile of the eight-story RC building among the three cases

Conclusions

A 3D linear FE method with an included water volume for examining the soil–building interaction based on a three-component input seismic wavefield was developed. In the new method, very soft soils are substituted for the water volume, so only solid material is treated, and wave propagation is controlled according to wave types in the very soft soils that replace the water volume. The method was applied to the reclaimed zone of Tokyo Bay.

The following can be concluded: (1) The method seems to work fairy well, judging from the soil responses evaluated for three cases prepared for confirming the effects of the method; (2) at the presence of the water volume, the soil responses become variable in the direction along which the soil volume is changed to the water volume; and (3) also, the building responses get larger in the same direction because the pile foundation has a certain extent in the horizontal directions.

Acknowledgments

The majority of the accelerograms employed to construct wavefields were provided as the data set of Strong Motion Array Observation No. 2 by the Association for Earthquake Disaster Prevention of Japan. Parts of the accelerograms of the Echujima station were supplied by Shimizu Corporation of Japan.

Notation

The following symbols are used in this paper:

$[C]$ = damping matrix;
$\{F\}$ = external force vector;
$[H_K]$ = matrix of the damping factors associated with the stiffness;
$[H_M]$ = matrix of the damping factors associated with the mass;
h_{Kij} = ij element of $[H_K]$;
h_{Mij} = ij element of $[H_M]$;
h_{WFij} = damping factor used in the new method for soil–building interaction;
$[K]$ = stiffness matrix;
$[M]$ = mass matrix;
M_J = earthquake magnitude;
p = external displacement contributed by body waves;
q = external displacement contributed by surface waves;
t = time;
Vp = P-wave velocity;
Vs = S-wave velocity;
$\{\chi\}$ = displacement vector associated with the system;
θ = vertical displacement;
ζ and η = horizontal displacements;
λ and μ = Lame's constants;

ρ = density; and
ω_1 = primary angular frequency of the ground.

References

Abdel-Ghaffar, A. M., and Elgamal, A. M. (1987). "Elasto-plastic seismic response of 3-D earth dams: Theory." *J. Geotechnical Eng.*, 10.1061/(ASCE)0733-9410(1987)113:11(1293), 1293–1308.

Abe, Y., et al. (1984). "Dynamic behavior of pile foundation during earthquakes." *Proc., 8th World Conf. Earthquake Engineering*, Prentice Hall, Upper Saddle River, NJ, 585–592.

Antes, H., and Estorff, O. V. (1987). "Analysis of absorption effects on the dynamic response of dam reservoir systems by boundary element methods." *Earthquake Eng. Struct. Dyn.*, 15(8), 1023–1036.

Bielak, J., and Christiano, P. (1984). "On the effective seismic input for non-linear soil-structure interaction systems." *Earthquake Eng. Struct. Dyn.*, 12(1), 107–119.

Building Center of Japan. (2013). *The building standard law of Japan (enforcement order of building standard law)*, Tokyo.

Chopra, A. K. (1968). "Earthquake behavior of reservoir-dam systems." *J. Engrg. Mech. Div.*, 94(6), 1475–1500.

Flores-Berrones, R., and Whitman, R. V. (1982). "Seismic responses of end-bearing piles." *J. Geotech. Engrg. Div.*, 108(4), 555–569.

Housner, G. W. (1957). "Interaction of building and ground during an earthquake." *Bull. Seismol. Soc. Am.*, 47(3), 179–186.

Housner, G. W. (1963). "The dynamic behavior of water tanks." *Bull. Seism. Soc. Am.*, 53(2), 381–387.

Iida, M. (2006). "Three-dimensional linear and simplified nonlinear soil response methods based on an input wave field." *Int. J. Geomech.*, 10.1061/(ASCE)1532-3641(2006)6:5(342), 342–355.

Iida, M. (2007). "Estimation of the wave fields in the three geotechnical zones of Tokyo." *Bull. Seism. Soc. Am.*, 97(2), 575–590.

Iida, M. (2013). "Three-dimensional finite-element method for soil-building interaction based on an input wave field." *Int. J. Geomech.*, 10.1061/(ASCE)GM.1943-5622.0000232, 430–440.

Iida, M. (2016). "Three-dimensional nonlinear soil response methods based on a three-component input wave field." *Int. J. Geomech.*, 10.1061/(ASCE)GM.1943-5622.0000482, 04015026.

Iida, M., and Hatayama, K. (2007). "Effects of seawater of Tokyo Bay on short-period strong ground motion." *Bull. Seism. Soc. Am.*, 97(4), 1324–1333.

Iida, M., Iiba, M., Kusunoki, K., Miyamoto, Y., and Isoda, H. (2015). "Seismic responses of two RC buildings and one wood building based on an input wave field." *Int. J. Geomech.*, 10.1061/(ASCE)GM.1943-5622.0000444, 04014093.

Iida, M., Yamanaka, H., and Yamada, N. (2005). "Wavefield estimated by borehole recordings in the reclaimed zone of Tokyo Bay." *Bull. Seism. Soc. Am.*, 95(3), 1101–1119.

Jaiswal, O. R., Rai, D. C., and Jain, S. K. (2007). "Review of seismic codes on liquid-containing tanks." *Earthquake Spectra*, 23(1), 239–260.

Larkin, T. (2008). "Seismic response of liquid storage tanks incorporating soil structure interaction." *J. Geotech. Geoenviron. Eng.*, 10.1061/(ASCE)1090-0241(2008)134:12(1804), 1804–1814.

Lysmer, J. M., and Kuhlemeyer, R. L. (1969). "Finite dynamic model for infinite media." *J. Engrg. Mech. Div.*, 95(4), 859–878.

Matsui, T., and Nagaya, T. (2015). "Nonlinear oscillation of a floating roof in a cylindrical tank under liquid sloshing: Model tests versus theoretical prediction." *J. Struct. Constr. Eng. Archit. Inst. Jpn.*, 80(710), 593–599.

Miura, F., and Wang, J. (1993). "Dynamic response analysis of structure-water-ground systems in the time domain using semi-infinite elements." *Proc. Japan Soc. Civil Eng.*, 471(I-24), 59–65.

Ohta, T., Niwa, M., and Ueno, K. (1978). "Seismic response characteristics of structure with pile foundation on soft subsoil layer." *Proc., 5th Japan Earthquake Eng. Symp.*, 561–568, Tokyo (in Japanese).

Sheil, B., and Finnegan, W. (2017). "Numerical simulations of wave-structure-soil interaction of offshore monopiles." *Int. J. Geomech.*, 10.1061/(ASCE)GM.1943-5622.0000667, 04016024.

Shija, N. P., and MacQuarrie, K. T. B. (2015). "Numerical simulation of active heat injection and anomalous seepage near an earth dam-concrete interface." *Int. J. Geomech.*, 10.1061/(ASCE)GM.1943-5622.0000432, 04014084.

Shiojiri, H., and Taguchi, T. (1985). "Development of a seismic response analysis method of concrete gravity dams—A method for time-domain nonlinear analysis of semi-infinite foundation-structure-water system." *Rep. No. 385012*, Electric Central Research Institute of Japan, Tokyo (in Japanese).

Syed, N. M., and Maheshwari, B. K. (2014). "Modeling using coupled FEM-SBFEM for three-dimensional seismic SSI in time domain." *Int. J. Geomech.*, 10.1061/(ASCE)GM.1943-5622.0000296, 118–129.

Touhei, T., and Ohmachi, T., (1990). "A FE-BE method in the time domain for dynamic response analysis of dam-foundation-reservoir systems." *Proc. Japan Soc. Civil Eng.*, 422(I-14), 381–390 (in Japanese).